Surface hopping outperforms secular Redfield theory when reorganization energies range from small to moderate (and nuclei are classical)

Brian R. Landry and Joseph E. Subotnik

Citation: The Journal of Chemical Physics **142**, 104102 (2015); doi: 10.1063/1.4913494
View online: http://dx.doi.org/10.1063/1.4913494
View Table of Contents: http://scitation.aip.org/content/aip/journal/jcp/142/10?ver=pdfcov
Published by the AIP Publishing

Surface hopping outperforms secular Redfield theory when reorganization energies range from small to moderate (and nuclei are classical)

Brian R. Landry[a] and Joseph E. Subotnik
Department of Chemistry, University of Pennsylvania, 231 S. 34th Street, Philadelphia, Pennsylvania 19104, USA

(Received 29 December 2014; accepted 12 February 2015; published online 9 March 2015)

We evaluate the accuracy of Tully's surface hopping algorithm for the spin-boson model in the limit of small to moderate reorganization energy. We calculate transition rates between diabatic surfaces in the exciton basis and compare against exact results from the hierarchical equations of motion; we also compare against approximate rates from the secular Redfield equation and Ehrenfest dynamics. We show that decoherence-corrected surface hopping performs very well in this regime, agreeing with secular Redfield theory for very weak system-bath coupling and outperforming secular Redfield theory for moderate system-bath coupling. Surface hopping can also be extended beyond the Markovian limits of standard Redfield theory. Given previous work [B. R. Landry and J. E. Subotnik, J. Chem. Phys. **137**, 22A513 (2012)] that establishes the accuracy of decoherence-corrected surface-hopping in the Marcus regime, this work suggests that surface hopping may well have a very wide range of applicability. © *2015 AIP Publishing LLC.* [http://dx.doi.org/10.1063/1.4913494]

I. INTRODUCTION

The study of nonadiabatic relaxation has become popular in recent years due to applications in alternative energy, molecular electronics, and spectroscopy. A complete theoretical study of such electronic relaxation is difficult because of the possibility of so many different and complex environments. For the standard spin-boson model[1,2] with a quantum-Brownian-oscillator spectral density, there are at least six different energy parameters that enter the calculation (the electronic coupling V, the system bath coupling which is proportional to the reorganization energy E_r, the driving force ϵ_0, temperature kT, friction $\hbar\gamma$, and a nuclear frequency $\hbar\Omega$). Thus, at least 6! different energy regimes are possible.

In practice, the two most studied parameter regimes are the Marcus limit (strong system-bath coupling) and the Redfield limit (weak system-bath coupling). On the one hand, for the Marcus limit, strong system-bath coupling leads to localization of the electronic state on one of the sites and the corresponding rate of electron transfer is the (Fermi-golden-rule) Marcus rate.[3] On the other hand, for the Redfield limit, weak system bath coupling can lead to electronic delocalization in an "excitonic" basis. If one further assumes that the bath has a short memory, one can derive the Markovian Redfield master equation for the density matrix of the electronic system.[4]

Now, many systems lie in an intermediate regime between the Marcus and the Redfield limits, where the system-bath coupling is of the same order as the electronic coupling, and there has been a substantial literature focusing on how to bridge these two limits. One early example was the "modified Redfield" idea of Chernyak and Mukamel *et al.*[5–7] Recently, the hierarchical equations of motions (HEOM) were developed by Ishizaki and Fleming[8] specifically to bridge the divide between the Redfield and Marcus limits. Other promising directions are a combination of master equations and polaron transformations, as advocated by Jang *et al.*,[9–11] and hybrid trajectory/density matrix approaches by Reichman,[12] Shi and Geva,[13,14] and Markland[15] and co-workers.

The list above has so far excluded Tully's fewest switches surface-hopping (FSSH) algorithm.[16] In recent years, the FSSH algorithm has become a very popular[17–19] tool for modeling electronic relaxation because (i) the algorithm is simple to implement, (ii) the algorithm can be applied formally with arbitrary Hamiltonians (i.e., not just a harmonic bath), and (iii) the algorithm recovers detailed balance up to a small correction.[20,21] Moreover, in a series of recent papers, we have shown that, provided decoherence[22–36] is properly treated,[37] an augmented FSSH algorithm (A-FSSH)[38,39] will recover the Marcus regime for electron transfer.[39] However, to our knowledge, the performance of the FSSH algorithm in the Redfield regime has not yet been investigated in the literature, presumably for two reasons. First, until recently, it was unclear how to initialize a surface hopping calculation over a linear combination of adiabatic states;[40] this conundrum has now been resolved.[41,42] Second, many researchers have likely presumed that FSSH must fail in the Redfield regime. After all, in the Redfield regime, electronic coherence is important (unlike the Marcus regime wherein wavepackets separate irreversibly) and FSSH cannot capture recoherences (wavepacket separation and recombination).[42] Despite this fear, however, there is also reason to suspect that FSSH might perform well in the Redfield regime: after all, in the limit of zero system-bath coupling, wavepacket separation will be minimal, no quantum feedback should be necessary, and all interesting dynamics should be entirely electronic.

With this context in mind, our goal here is to analyze the performance of the FSSH algorithm starting deep in the Redfield limit as a function of increasing reorganization energy. We

[a]Electronic mail: landrybr@gmail.com

will show that FSSH does obtain quite reasonable rates in the Redfield regime as long as the temperature is large enough that nuclear motion is classical. Thus, surface hopping methods are applicable in two extreme limits (Redfield and Marcus), and we will hypothesize that these methods may well be applicable over a large range of parameter regimes in between.

Our test system will be the standard spin-boson model. The spin-boson model consists of a two level (electronic) system, linearly coupled to a bath Hamiltonian made up of a large number of harmonic oscillators. Using Pauli matrices, the Hamiltonian for this system can be written as

$$H = H_S + H_B + H_I, \tag{1}$$

$$H_S = \frac{\epsilon_0}{2}\sigma_z + V\sigma_x, \tag{2}$$

$$H_B = \sum_\alpha \frac{{p_\alpha}^2}{2m} + \frac{1}{2}m_\alpha {\omega_\alpha}^2 {x_\alpha}^2, \tag{3}$$

$$H_I = \sum_\alpha c_\alpha x_\alpha \sigma_z. \tag{4}$$

The interaction Hamiltonian is characterized by the set of coupling constants $\{c_\alpha\}$ which define the spectral density,

$$J(\omega) = \frac{\pi}{2}\sum_\alpha \frac{{c_\alpha}^2}{m_\alpha\omega_\alpha}\delta(\omega - \omega_\alpha). \tag{5}$$

One measure of the overall strength of the interaction between the system and bath is the reorganization energy,

$$E_r = \frac{4}{\pi}\int_0^\infty d\omega \frac{J(\omega)}{\omega}. \tag{6}$$

Here, we will use a simple spectral density: the quantum Brownian oscillator

$$J(\omega) = \frac{1}{2}\frac{E_r\Omega^2\gamma\omega}{(\omega^2-\Omega^2)^2 + \gamma^2\omega^2}. \tag{7}$$

In practice, Eq. (7) is equivalent to the case whereby the quantum degree of freedom is coupled to a single classical coordinate q which is subject to classical Langevin dynamics (i.e., a random force and damping term γ). More formally, the mode q is coupled to a bath of nuclear coordinates y_α with momenta π_α. The corresponding Hamiltonian is

$$\begin{aligned} H_B &= \frac{p^2}{2M} + \frac{1}{2}M\Omega^2 q^2 \\ &\quad + \sum_\alpha \frac{{\pi_\alpha}^2}{2m_\alpha} + \frac{1}{2}m_\alpha {\omega_\alpha}^2 {y_\alpha}^2 + d_\alpha y_\alpha q, \\ H_I &= \lambda q\sigma_z. \end{aligned} \tag{8}$$

Here, λ is related to the reorganization energy E_r in Eq. (7) according to $\lambda = \sqrt{E_r M\Omega^2/2}$, and we have set

$$J_{osc}(\omega) \equiv \frac{\pi}{2}\sum_\alpha \frac{{d_\alpha}^2}{m_\alpha\omega_\alpha}\delta(\omega-\omega_\alpha) = M\gamma\omega. \tag{9}$$

The Ohmic form of Eq. (9) ensures that the random force on coordinate q will be a memoryless (delta-correlated) Langevin force.

II. THEORETICAL METHODS

In the Redfield regime, the reorganization energy is the small parameter and it is prudent to consider the basis that diagonalizes the system Hamiltonian alone, the exciton basis. In such a basis, the bath Hamiltonian (H_B) is unchanged, and the system and system-bath Hamiltonians are

$$H_S = \sigma_z\sqrt{\left(\frac{\epsilon_0}{2}\right)^2 + V^2}, \tag{10}$$

$$H_I = \sum_\alpha \frac{c_\alpha x_\alpha}{\sqrt{\left(\frac{\epsilon_0}{2}\right)^2 + V^2}}\left(\frac{\epsilon_0}{2}\sigma_z + V\sigma_x\right). \tag{11}$$

Below, we will study the populations and coherences of the system as a function of time in the "exciton basis" using several different approaches.

A. Surface hopping, Ehrenfest, and no feedback (NF) quasi-1D dynamics

First, we ran FSSH, A-FSSH,[43] Ehrenfest, and no feedback dynamics to model diabatic populations and coherences. For these simulations, we used only a single Brownian oscillator, with a friction parameter γ, coupled to a quantum (electronic) degree of freedom (i.e., the Hamiltonian in Eq. (8)). Stochastic 1D dynamics are equivalent to the deterministic dynamics of a set of many oscillators with the spectral density in Eq. (7).[44–46] Note that, for a mixed quantum-classical description to hold, the special harmonic coordinate q must undergo classical dynamics, which is true as long as $kT \geq \hbar\Omega$. For the NF dynamics, all trajectories are propagated classically on the average surface with force $1/2\,(F_{11} + F_{22})$ (here F_{11} and F_{22} are the ground and excited adiabatic state forces).

B. Redfield rate

Second, dynamics were investigated using the secular Redfield relaxation equations. Formally, the Redfield limit requires two separate conditions: (1) The interaction between the system and bath must be weak; this leads to the condition $V \gg E_r$ where V is the diabatic coupling. (2) The bath relaxation time should be very fast so that memory effects can be ignored (the Markov approximation). This condition of fast bath relaxation presupposes that the frequencies of the bath oscillators (that are most important in the coupling to the system) must be larger than any system timescale. This condition can be summed up as $\frac{\Omega^2}{\gamma} \gg \frac{V}{\hbar}$.

In this limit of weak system-bath interaction and fast bath relaxation, the time evolution of the system density matrix can be calculated analytically. Within the secular approximation, the rates of population decay, $1/T_1$, and coherence decay, $1/T_2$, depend only on the real part of the golden rule expressions. Carrying out the relevant integrals and averages from these golden rule expressions gives the Redfield population and coherence decay rates

$$\begin{aligned} \frac{1}{T_1} &= \frac{E_r\Omega^2}{\hbar}\left(\frac{V^2}{(\epsilon_0/2)^2 + V^2}\right)\coth\left(\frac{\sqrt{\epsilon_0^2 + 4V^2}}{2kT}\right) \\ &\quad \times \frac{\gamma\hbar^3\sqrt{\epsilon_0^2 + 4V^2}}{(\epsilon_0^2 + 4V^2 - \hbar^2\Omega^2)^2 + \hbar^2\gamma^2(\epsilon_0^2 + 4V^2)}, \end{aligned} \tag{12}$$

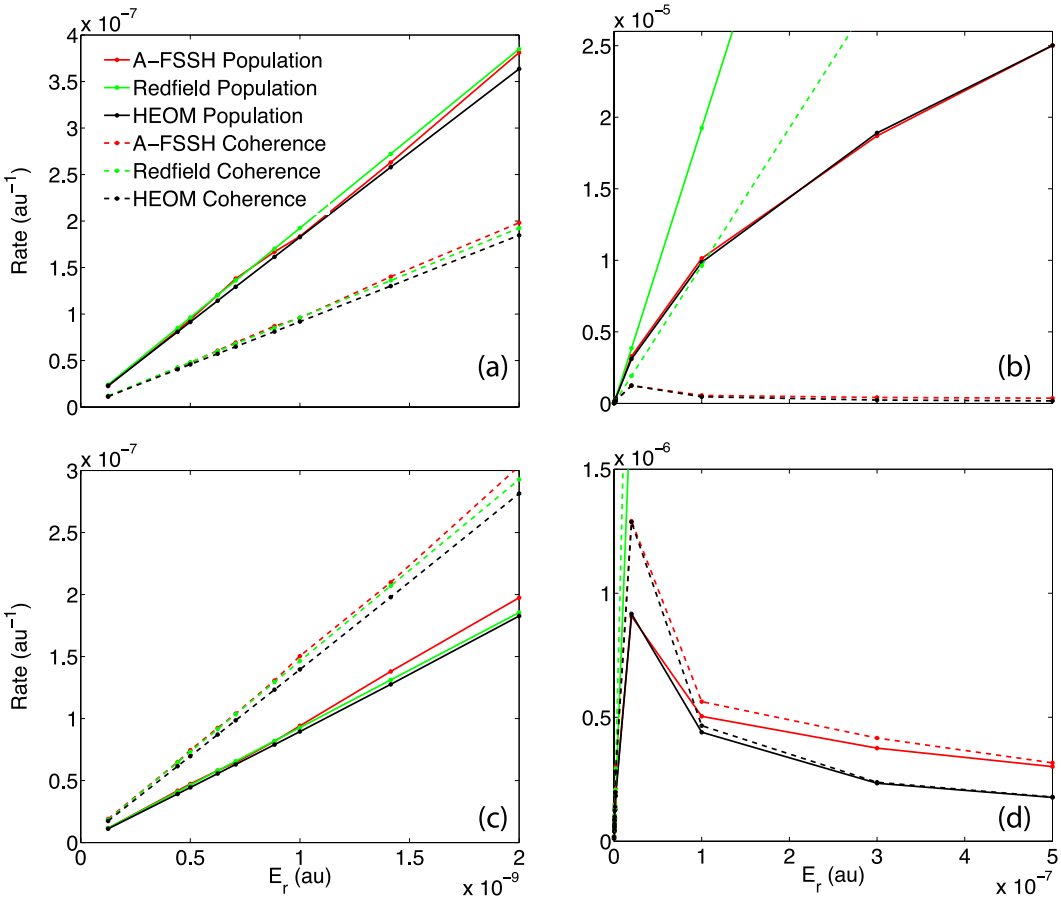

FIG. 1. $1/T_1$ and $1/T_2$ for the spin-boson system with $\epsilon_0 = 0$ in (a) and (b) and $\epsilon_0 = 2V$ in (c) and (d). Other parameters (in atomic units): $V = 10^{-6}$, $\Omega = 10^{-4}$, $kT = 10^{-3}$, and $\gamma = 10^{-3}$. Ehrenfest, NF, and FSSH dynamics are all close to HEOM (not shown). The range of accuracy for secular Redfield theory is very limited in this high temperature regime (even when no quantum feedback is necessary); secular Redfield theory fails unless $E_r \ll 0.04V$.

$$\frac{1}{T_2} = \frac{1}{2T_1} + \frac{1}{T_2^*}, \tag{13}$$

$$\frac{1}{T_2^*} = \frac{E_r\gamma}{2\hbar^2\Omega^2}\left(\frac{\epsilon_0^2}{(\epsilon_0/2)^2 + V^2}\right)kT. \tag{14}$$

C. HEOM

Our third approach for calculating relaxation rates is the HEOM.[8,47] HEOM is a powerful tool for solving for the time evolution of the spin (system) density matrix as evolved by the Hamiltonian (Eq. (1)) provided that the spectral density takes a Drude form. HEOM succeeds by taking advantage of the special form of the correlation function associated with a Drude spectral density.

The most general Drude spectral density is given by

$$J(\omega) = 2\lambda_D\left(\frac{\gamma_D\omega}{\omega^2 + {\gamma_D}^2}\right). \tag{15}$$

In order to best compare many dimensional HEOM results with 1D surface hopping results, we must make an identification of the Brownian spectral density (Eq. (7)) with the Drude spectral density (Eq. (15)). This is possible in the limit $\Omega \gg \omega$. In this limit, the Brownian spectral density becomes

$$J(\omega) = \frac{1}{2}\frac{E_r\frac{\Omega^2}{\gamma}\omega}{\left(\frac{\Omega^2}{\gamma}\right)^2 + \omega^2} \tag{16}$$

and it is possible to identify γ_D and λ_D with values from the Brownian spectral density as follows:

$$\gamma_D = \frac{\Omega^2}{\gamma}, \tag{17}$$

$$\lambda_D = \frac{E_r}{4}. \tag{18}$$

Now, in order to insist that $\Omega \gg \omega$ for all possible frequencies ω, we require that Ω be much greater than the largest frequencies sampled in the spectral density. This cutoff frequency is γ_D. Therefore, in order to make the identification between the Drude and Brownian spectral densities, we require $\Omega \gg \gamma_D$ (i.e., $\gamma \gg \Omega$ in Eq. (7)).

D. Rate extraction

For the surface hopping, Ehrenfest, and HEOM calculations, rates can be calculated by fitting a dynamical observable $a(t)$ to be of the form $a(t) \approx a_0 + a_1\exp(-bt)$. We then define b to be the rate. Surface hopping, Ehrenfest, and no feedback results sampled approximately 10 000 trajectories each.

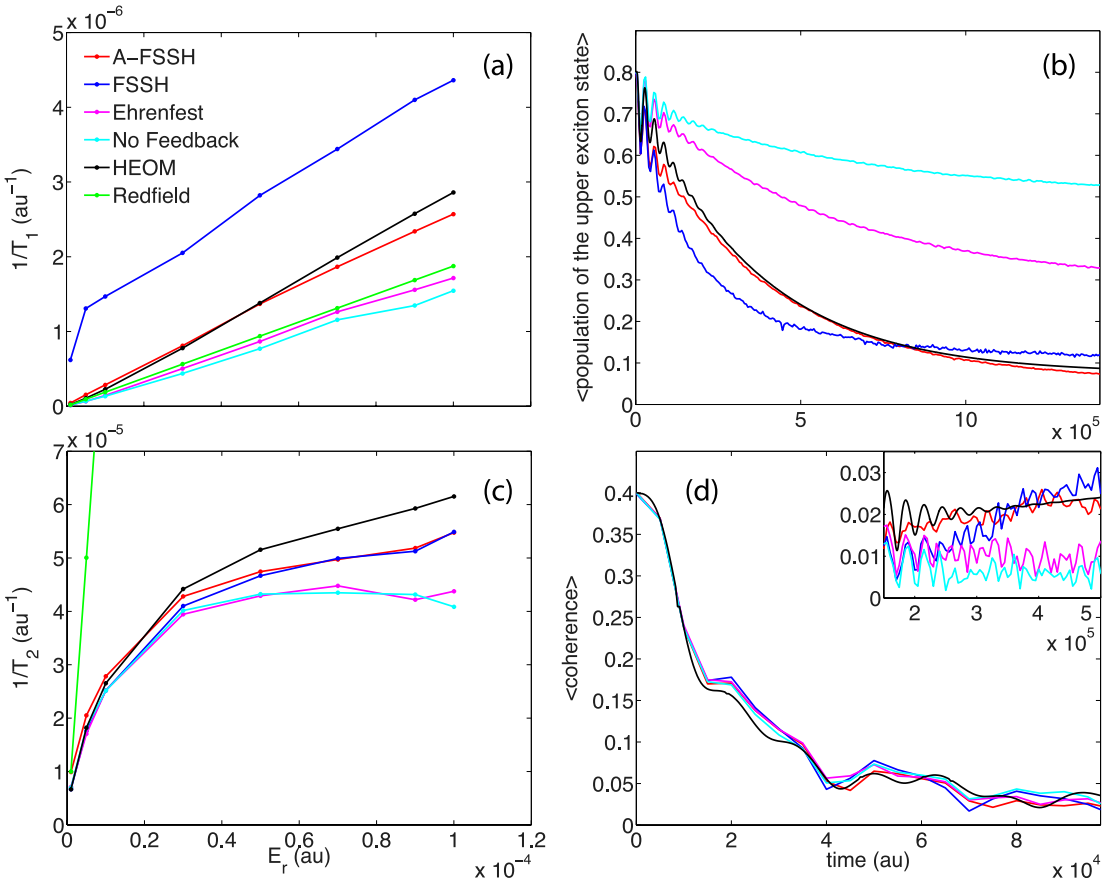

FIG. 2. (a) Plot of $1/T_1$ for the spin-boson system. (b) The corresponding population decay for $E_r = 10^{-4}$. (c) Plot of $1/T_2$ for the spin-boson system. (d) The corresponding coherence decay for $E_r = 10^{-4}$. The inset plots coherence at long times; note that only FSSH and A-FSSH recover the correct long time limit. Parameters (in atomic units): $V = 10^{-4}$, $\Omega = 10^{-4}$, $kT = 10^{-4}$, $\epsilon_0 = 2\times10^{-4}$, and $\gamma = 10^{-3}$. These parameters do not satisfy the Markovian approximation in Redfield theory, i.e., we set $V \gg \hbar\Omega^2/\gamma$, and thus standard Redfield theory is not expected to apply.

III. RESULTS AND DISCUSSION

We will now study the dynamics that occur after starting in the Redfield regime and increasing E_r. To identify HEOM results with a 1-D stochastic model, we will restrict ourselves to the case that $\gamma \gg \Omega$; for classical mechanics to remain accurate, we will also restrict ourselves to the case that $kT \geq \Omega$.

A. High temperature

Figure 1 shows population and coherence decay rates starting from an initial system density matrix[48] (in the exciton basis),

$$\rho_0 = \begin{pmatrix} 0.2 & 0.4 \\ 0.4 & 0.8 \end{pmatrix} \tag{19}$$

and an uncoupled bath in equilibrium. (Here, the basis is ordered such that the first state $|1\rangle$ has lower energy than the second state $|2\rangle$.) We plot decay rates for HEOM (exact), A-FSSH, and Redfield; Ehrenfest, NF, and FSSH dynamics are all close to HEOM (not shown). In Fig. 1(a), we set $\epsilon_0 = 0$ (no bias between wells) and in Fig. 1(c), we set $\epsilon_0 = 2V$. Clearly, for this regime, the temperature is large enough that no quantum feedback is necessary.

Note that, for $\epsilon_0 = 0$, the coherence decay is slower than the population decay because there is no pure dephasing rate ($1/T_2^* = 0$). However, for $\epsilon_0 = 2V$, the situation reverses itself and now the coherence decay is faster than the population decay (because $1/T_2^* > 0$). All semiclassical rates agree with secular Redfield theory in Figs. 1(a) and 1(c). Interestingly, this reversal in relevant rates and the possibility that $T_2 = 2T_1$ are predicted by any and all classical schemes (FSSH, NF, Ehrenfest, etc.); there are no important nonadiabatic effects for the quantum dynamics of the nuclei.

In Figs. 1(b) and 1(d), we extend parts *a* and *c* to include larger values of E_r comparable to V. One quickly realizes the limitations of secular Redfield theory, which has the completely incorrect behavior as soon as $E_r \geq 0.04V$. In other words, for accuracy, secular Redfield theory requires the small parameter E_r/V to be *very* small, less than 0.04. By contrast, all semiclassical methods continue to agree pretty well with HEOM over a much broader range of parameters. Admittedly, A-FSSH has a small error (note the scale) compared with HEOM and FSSH, suggesting that our decoherence correction is slightly too large in this regime. Overall, though, all semiclassical methods nearly agree and vastly outperform secular Redfield theory at high temperature.

Before discussing our next example, we note that this failure of Redfield theory is not the direct result of a Markovian

breakdown, as the electronic coupling is much less than the characteristic bath frequency ($V = 1 \times 10^{-6} \ll \hbar\Omega^2/\gamma = 1 \times 10^{-5}$). We also note that full Redfield theory (without the secular approximation, not shown) does not correct the problems above for secular Redfield theory. To be specific, full Redfield theory will make a large correction only for the rate of coherence decay when $\epsilon_0 = 0$ in Fig. 1(b). However, for all other curves in Fig. 1, full Redfield theory creates only minor changes relative to the secular approximation.

B. Finite temperature

Next, we lower the temperature of our simulation and explore the limit $E_r \to V$ in order to more thoroughly test the surface hopping algorithms. In such a case, one needs to include quantum feedback on the nuclear motion for accurate answers. To make the simulation most difficult, we will choose parameters that are all close in value and explore the dynamics as a function of lowering E_r. These parameters will not obey a Markovian approximation for the nuclear bath, i.e., we will choose $V \gg \hbar\Omega^2/\gamma$. In such a case, Redfield theory is likely to fail, but it will be interesting to analyze the performance of surface hopping techniques when there is no obviously small parameter.

In Figs. 2(a) and 2(c), we plot population and coherence decay rates, respectively, as a function of reorganization energy. From the data, it is clear that, as compared with HEOM data, the best semiclassical approach is the A-FSSH algorithm. Without decoherence, FSSH overestimates the population decay rate while Ehrenfest dynamics underestimates the population decay rate. With a decoherence correction on top of FSSH, A-FSSH gives the best estimate of the population decay rate. As for the coherence decay rates, FSSH and A-FSSH yield similar answers that are close to the HEOM results, while Ehrenfest dynamics underestimates the coherence decay rate. Interestingly, Ehrenfest results mimic results without any quantum feedback. Perhaps surprisingly, the secular Redfield rates agree with Ehrenfest dynamics for the population decay–but, perhaps unsurprisingly, the secular Redfield rates are wildly inaccurate for the coherence decay rate.

Finally, in Figs. 2(b) and 2(d), we plot the population and coherence as a function of time for $\epsilon_0 = 2V$. These plots remind us that, even though they may yield reasonable rates, Ehrenfest and NF dynamics will not recover the correct equilibrium populations or coherences at long times (which is a major limitation of these methods); by contrast, FSSH and A-FSSH do recover the correct long time limits. Moreover, we observe that A-FSSH does recover both the early time oscillations as well as long time decay rates; clearly, our decoherence correction improves FSSH results even when E_r is not that big. Overall, Fig. 2 offers a firm validation of the surface hopping approach in this range of weak to moderate system-bath coupling.[49]

IV. CONCLUSIONS

The data above demonstrate that surface hopping methods work well for the regime of weak to moderate system-bath couplings. In the limits of extremely weak system-bath coupling, A-FSSH and FSSH are the same algorithm and both agree with exact results for a trivial reason: no quantum feedback is necessary and wavepackets never separate much. As the system-bath coupling increases, a decoherence correction does become necessary for FSSH dynamics, and A-FSSH behaves well. Now, given the success of A-FSSH dynamics in reproducing nonadiabatic Marcus theory[39] in the limit of large system-bath couplings, we conclude that decoherence-corrected surface hopping succeeds in two opposing regimes and would appear to be a strong candidate for dealing with open quantum systems over a large range of parameter regimes.

Future studies are now needed for assessing exactly where surface hopping fails—beyond the limit of low temperatures where classical mechanics fails, there will also be those particular regimes (and, specifically, spectral densities) where wavepackets separate and then recombine and the validity of surface hopping will be very questionable. How common are these intermediate regimes?[9,50–52] And will these regimes limit the *experimental* applicability of FSSH in practice? Only time will tell.

ACKNOWLEDGMENTS

This material is based upon work supported by the (U.S.) Air Force Office of Scientific Research (USAFOSR) PECASE award under AFOSR Grant No. FA9950-13-1-0157. We thank Seogjoo Jang for helpful and stimulating conversations.

[1] A. Caldeira and A. Leggett, Phys. A **121**, 587 (1983).
[2] A. Leggett, S. Chakravarty, A. Dorsey, M. Fisher, A. Garg, and W. Zwerger, Rev. Mod. Phys. **59**, 1 (1987).
[3] A. Nitzan, *Chemical Dynamics in Condensed Phases* (Oxford University Press, USA, 2006).
[4] K. Blum, *Density Matrix Theory and Applications* (Plenum Press, New York, 1996).
[5] T. Meier, V. Chernyak, and S. Mukamel, J. Chem. Phys. **107**, 8759 (1997).
[6] W. M. Zhang, T. Meier, V. Chernyak, and S. Mukamel, J. Chem. Phys. **108**, 7763 (1998).
[7] M. Yang and G. R. Fleming, Chem. Phys. **275**, 355 (2002).
[8] A. Ishizaki and G. R. Fleming, J. Chem. Phys. **130**, 234111 (2009).
[9] S. Jang, T. C. Berkelbach, and D. R. Reichman, New J. Phys. **15**, 105020 (2013).
[10] S. Jang, Y. C. Cheng, D. R. Reichman, and J. D. Eaves, J. Chem. Phys. **129**, 101104 (2008).
[11] S. Jang, J. Chem. Phys. **131**, 184102 (2009).
[12] T. C. Berkelbach, T. E. Markland, and D. R. Reichman, J. Chem. Phys. **136**, 084104 (2012).
[13] Q. Shi and E. Geva, J. Chem. Phys. **119**, 12063 (2003).
[14] Q. Shi and E. Geva, J. Chem. Phys. **120**, 10647 (2004).
[15] A. Kelly and T. E. Markland, J. Chem. Phys. **139**, 014104 (2013).
[16] J. C. Tully, J. Chem. Phys. **93**, 1061 (1990).
[17] D. Nachtigallova, A. J. A. Aquino, J. J. Szymczak, M. Barbatti, P. Hobza, and H. Lischka, J. Phys. Chem. A **115**, 5247 (2011).
[18] W. R. Duncan and O. V. Prezhdo, Annu. Rev. Phys. Chem. **58**, 143 (2007).
[19] T. Nelson, S. Fernandez-Alberti, A. E. Roitberg, and S. Tretiak, Acc. Chem. Res. **47**, 1155 (2014).
[20] P. V. Parandekar and J. C. Tully, J. Chem. Phys. **122**, 094102 (2005).
[21] J. R. Schmidt, P. V. Parandekar, and J. C. Tully, J. Chem. Phys. **129**, 044104 (2008).
[22] O. V. Prezhdo and P. J. Rossky, J. Chem. Phys. **107**, 825 (1997).
[23] M. J. Bedard-Hearn, R. E. Larsen, and B. J. Schwartz, J. Chem. Phys. **123**, 234106 (2005).
[24] R. E. Larsen, M. J. Bedard-Hearn, and B. J. Schwartz, J. Phys. Chem. B **110**, 20055 (2006).
[25] J. Y. Fang and S. Hammes-Schiffer, J. Phys. Chem. A **103**, 9399 (1999).
[26] J. Y. Fang and S. Hammes-Schiffer, J. Chem. Phys. **110**, 11166 (1999).
[27] Y. L. Volobuev, M. D. Hack, M. S. Topaler, and D. G. Truhlar, J. Chem. Phys. **112**, 9716 (2000).

[28]M. D. Hack and D. G. Truhlar, J. Chem. Phys. **114**, 2894 (2001).
[29]A. W. Jasper, M. D. Hack, and D. G. Truhlar, J. Chem. Phys. **115**, 1804 (2001).
[30]C. Zhu, A. W. Jasper, and D. G. Truhlar, J. Chem. Phys. **120**, 5543 (2004).
[31]C. Zhu, S. Nangia, A. W. Jasper, and D. G. Truhlar, J. Chem. Phys. **121**, 7658 (2004).
[32]A. W. Jasper and D. G. Truhlar, J. Chem. Phys. **123**, 064103 (2005).
[33]F. Webster, P. J. Rossky, and R. A. Friesner, Comput. Phys. Commun. **63**, 494 (1991).
[34]F. Webster, E. T. Wang, P. J. Rossky, and R. A. Friesner, J. Chem. Phys. **100**, 4835 (1994).
[35]K. F. Wong and P. J. Rossky, J. Chem. Phys. **116**, 8418 (2002).
[36]K. F. Wong and P. J. Rossky, J. Chem. Phys. **116**, 8429 (2002).
[37]B. R. Landry and J. E. Subotnik, J. Chem. Phys. **135**, 191101 (2011).
[38]J. E. Subotnik and N. Shenvi, J. Chem. Phys. **134**, 024105 (2011).
[39]B. R. Landry and J. E. Subotnik, J. Chem. Phys. **137**, 22A513 (2012).
[40]U. Muller and G. Stock, J. Chem. Phys. **107**, 6230 (1997).
[41]B. R. Landry, M. J. Falk, and J. E. Subotnik, J. Chem. Phys. **139**, 211101 (2013).
[42]J. E. Subotnik, W. Ouyang, and B. R. Landry, J. Chem. Phys. **139**, 214107 (2013).
[43]We used Eq. 11 of Ref. 41 to determine the diabatic populations and coherences.
[44]S. Mukamel, *Principles of Nonlinear Optical Spectroscopy* (Oxford University Press, New York, 1995).
[45]A. Garg, J. N. Onuchi, and V. Ambegaokar, J. Chem. Phys. **83**, 4491 (1985).
[46]W. Xie, S. Bai, L. Zhu, and Q. Shi, J. Phys. Chem. A **117**, 6196 (2013).
[47]J. Strümpfer and K. Schulten, J. Chem. Theory Comput. **8**, 2808 (2012).
[48]We consistently find the same results if we study different initial conditions of the density matrix, e.g., $\rho_0 = \begin{pmatrix} 0.3 & \sqrt{0.21} \\ \sqrt{0.21} & 0.7 \end{pmatrix}$.
[49]Although the A-FSSH decoherence approximation arises from an expansion of the position and momentum moments around a FSSH trajectory, it is important to remember that the accuracy of this correction does not depend on harmonic potential energy surfaces. In particular, we emphasize that, within the A-FSSH algorithm, the second derivative of the potential energy is completely ignored and never used for the moment calculations. Thus, while a moment expansion would terminate formally at a second order with the assumption of harmonic potential energy surfaces, the A-FSSH calculation is in fact terminated earlier, at first order. Thus, the spin-boson problem is indeed a strong test of the A-FSSH decoherence correction. Moreover, because the QCLE is exact for the spin-boson problem, any failures of the FSSH algorithm must arise from failures of the decoherence correction applied by A-FSSH.
[50]J. Wu, F. Liu, Y. Shen, J. Cao, and R. J. Silbey, New J. Phys. **12**, 105012 (2010).
[51]M. Mohseni, P. Rebentrost, S. Lloyd, and A. Aspuru-Guzik, J. Chem. Phys. **129**, 174106 (2008).
[52]I. Kassal and A. Aspuru-Guzik, New J. Phys. **14**, 053041 (2012).